Impact of Ambient Temperature and Humidity on the Performance of Vapour Compression Air Conditioning System - Experimental and Numerical Investigation

Andrew N. Aziz[1,2,*], Saad Mahmoud[1], Raya Al-Dadah[1], Mohamed A. Ismail[3,4], Mohammed K. Almesfer[3]

1 Department of Mechanical Engineering, University of Birmingham, Edgbaston, Birmingham B15 2TT, United Kingdom
2 City of Scientific Research and Technological Applications, SRTA-City, New Borg El Arab City, 21934 Alexandria, Egypt
3 Department of Chemical Engineering, College of Engineering, King Khalid University, Abha 61411 Kingdom of Saudi Arabia
4 Institute of Engineering Research and Materials Technology, National Center for Research, Khartoum 2424, Sudan

ARTICLE INFO	ABSTRACT
  	Due to global warming, population growth, and urbanisation, demands for space cooling in buildings have significantly increased. Mechanical vapour compression cooling technology is relatively mature, well-understood and most commonly used globally. However, they suffer from high energy consumption and adverse environmental impact due to the refrigerants used. As ambient temperature and humidity have significant effects on the performance of vapour compression systems, this paper experimentally and numerically investigates their impact on the performance of vapour compression air conditioning system in terms of power consumption and cooling capacity. It was concluded that at ambient humidity of 55%, as the ambient temperature increases from 22 °C to 40 °C, the compressor temperature has increased from 46 °C to 59 °C which increased its power consumption from 751.2 to 935.52 Watts, giving an increase of 10.24 Watts for every one degree of ambient temperature increase. Also, as ambient humidity in-creased from 32% to 88%, the power consumption increased from 739.2 Watts to 853.2 Watts, an increase of 114 Watts. A validated CFD (Computational Fluid Dynamics) model was developed and predicted a loss in the enthalpy change from 11.7kJ/kg.d.a to 3.6kJ/kg.d.a. due to ambient temperature increasing from 22 °C to 40 °C and a loss of enthalpy change from 12.857kJ/kg.d.a to 5.524kJ/kg.d.a. due to increasing the ambient air humidity from 32% to 88%. This work high-lighted the impacts of ambient conditions on the performance of vapour compression cooling system in terms of increased power consumption and loss of cooling capacity.

1. Introduction

Rising temperatures, economic development, population growth and urbanisation have led to a significant increase in global demand for space cooling. The energy consumption for space cooling

---

* *Corresponding author.*
E-mail address: andrewnabil.dr18@gmail.com (Andrew N. Aziz)

has risen at an average pace of 4% per year since 2000, where the number of cooling units in operation has more than doubled since 2000, reaching over 2.2 billion units in 2021[1].

The International Energy Agency (IEA) predicted that commercial and domestic space cooling will account for 37% of the global electricity demand by 2050 and may match that of heating by 2060. Also, cooling in buildings, industrial processes, and supply chains accounts for 7% of global greenhouse gas emissions (GHGs) from energy consumption and the use of refrigerants, compared with around 2% from the aviation sector [2]. Currently, mechanical Vapour Compression (VCC) systems are dominant over air conditioning industry, a relatively mature and well-understood technology, but with intensive energy consumption and environmental issues [3, 4]. The VCC refrigeration system consists of four main components: compressor, condenser, expansion device, and evaporator, which are connected to produce the refrigeration effect through thermodynamic processes of compression, condensation, expansion, and evaporation [5, 6]. There are many thermodynamic losses associated with the operation of vapour compression that need to be addressed to provide high system performance, including constant enthalpy expansion due to high discharge temperature of the refrigerant, large power consumptions, rise in the condenser heat rejection, large throttling losses and drop in refrigeration capacity[7, 8]. Shah *et al.,* carried out a survey of the global air conditioning market revealing that the average efficiency of the sold air conditioners is less than half compared to the top expensive air-conditioning units [9]. Generally, the compression work for the VCC units is relatively high, particularly in the case for hot and dry climates, where the standard VCC systems experience significant efficiency drop due to high condenser temperatures leading to higher compression power consumption. Published data indicated that the coefficient of performance (COP) of the VCC systems decreases by 2-4% for every 1 °C increase in the condenser temperature [10].

Ambient temperature and humidity have significant effects on the performance of Vapour Compression systems, particularly in air conditioning and refrigeration applications in terms of cooling capacity and power consumption [11-13]. Higher ambient temperatures can limit the performance of the vapour compression system in terms of its cooling capacity, energy efficiency and increased compressor load [14-16]. The cooling capacity of a Vapour Compression system is adversely affected by the temperature difference between the ambient air and the space to be cooled. As the ambient temperature rises, the temperature differential decreases, and becomes more difficult to reject heat to a hotter environment leading to reduced cooling capacity. Yusof *et al.,* [17] carried out experimental work using small capacity split-unit air conditioner with R-22 refrigerant to study the effect of outdoor temperature on the performance of the air conditioner. They concluded that the highest cooling capacity was obtained at 100% refrigerant charge for all outdoor temperatures, and the cooling capacity dropped by 3.7% as the outdoor temperature increased from 30 °C to 36 °C. Setyawan *et al.,* [18] experimentally investigated the performance of 2.6 kW cooling capacity air conditioner using R32 with outdoor temperature varied from 24 to 36℃ while maintaining the humidity ratio at 14.9 kg vapour per 1 kg of dry air. They concluded that as the outdoor air temperature increased by 1℃, the power input increased by 1.4%, the cooling capacity decreased by 0.9%, and the coefficient of performance decreased by 1.95%. Yau et.al [19] used numerical investigation for a split air-cooled ducted blower (ADB) air conditioner in an office building located in Malaysia. They concluded that for every 1 °C increment in the outdoor temperature the total cooling capacity of the ADB system was reduced by 2%.

The energy efficiency of a vapour compression system is generally measured by its coefficient of performance (COP), which is the ratio of the provided cooling to the amount of electrical energy consumed. Increased ambient temperatures result in decreased COP values, as the system needs to work harder to transfer heat to a hotter environment, leading to higher energy consumption and

reduced efficiency. Xiea *et al.,* [20] developed a mathematical model for a vapour compression cooling system and investigated the impact of increased ambient temperature on the system performance. Simulations results showed that when ambient air temperature increased from 36ć to 45ć, the system COP decreased by 17.3%. Khalifa *et al.,* [21]conducted an experimental study on a window air conditioner using refrigerant R407C by varying ambient temperature from 30 to 50°C and concluded that the ambient temperature increases, the condenser heat rejection decreased by about 9.5% and COP decreased by 16%. Setyawan *et al.,* [22] carried out experimental study on a vapour compression air conditioner by varying ambient air dry-bulb temperature, and concluded that for every 1°C increase in outside temperature, the input power increased by 1.4%, and COP decreased by 2.0%. Also, height ambient temperatures can increase the workload on the air conditioner compressor, where it must operate at higher pressures to achieve the desired cooling effect, leading to additional stress and potential efficiency losses. Additionally, higher ambient temperatures can increase the risk of compressor overheating, which may cause system failures if not properly managed. Bilgili *et al.,* [23] present an experimental investigation on a typical residential split air conditioning system with ambient temperatures varying from 20 °C to 46 °C. Their results showed that as the ambient temperature increased from 20 °C to 46 °C, the pressure difference between the suction and discharge sections of the compressor has increased from 9.78 bar at 20 °C to 18.59 bar at 46 °C, and the compressor load increased from 0.380 kW to 0.589 kW. The compression ratio (CR) is defined as the ratio of the pressure at the outlet of the compressor to the pressure at the inlet. When the load on a compressor increases from higher ambient temperature, the CR increases accordingly, indicating higher power consumption and lower performance [24-26]. This is because the compressor must work harder to compress the refrigerant with higher pressure inlet, and the pressure at the outlet may not increase as much as it would under lower ambient temperatures.

Increased ambient humidity can have an adverse effect on the performance of the evaporator and the condenser of the vapour compression cooling systems, thus reducing its performance [27-31]. The condenser plays a significant role in rejecting heat to the surroundings, but when the ambient air is already saturated with moisture, it will have a lower capacity to absorb the heat released by the condenser. This reduces the effectiveness of condenser heat transfer, and the overall efficiency of the system and can lead to higher energy consumption. Also, the presence of moisture in the air affects the heat transfer coefficient between the condenser surfaces and the passing air. Water vapour has lower thermal conductivity compared to dry air, which reduces the heat transfer rate. This will lead to reduced system efficiency since the condenser will need to operate at higher temperatures to achieve the desired cooling effect. Similarly, when the air passing the evaporator coil is already saturated with moisture, it decreases the evaporator ability to absorb heat from the space being cooled. This reduces the system cooling capacity produce inadequate cooling. Therefore, high ambient humidity can result in increased energy consumption due to reduced system efficiency and cooling capacity. Computational Fluid Dynamics (CFD) is important for predicting and monitoring temperature and humidity levels in buildings, especially when integrated into desiccant systems CFD allows us to accurately model, and calculate, airflow and heat transfer room type, ventilation, and water source accounts. These technologies help optimize building design, HVAC design, and dry systems, ensure energy efficiency and comfort in buildings and improve the quality and efficiency of integrating CFD into dry systems is a powerful tool in modern building design and environmental engineering [32-34].

In order to optimise the performance of the vapour compression cooling system, it is essential to understand the effects of these ambient conditions on the system operation so that measures can be taken to improve its performance and reduce its energy consumption. This work experimentally

and numerically investigates the effects of ambient temperature and humidity on the performance of the VCC air condition system in terms of power consumption and cooling performance.

2. Experimental Setup

Figure 1 shows the experimental test facility used to investigate the effect of ambient temperature and humidity on the performance of an air conditioning system. It consists of a fully insulated room [35] with a volume of 2.2 m^3 connected with the vapour compression air conditioner by a 15cm circular duct. The air conditioner is from Climachil LTD with model number PAC15H, it has a cooling capacity of 15000 BTU/h and uses R410A as the refrigerant. The air conditioner consists of an evaporator, condenser, compressor and capillary tube. Figure 2a shows a photograph of the evaporator, it is a fin and tube heat exchanger with a tube outer diameter of 5mm and inner diameter of 4mm and length of 19.9 m, a number of fins of 8 fins/cm and a total fin area of 2.25 m^2, total surface area of 2.616 m^2. The evaporator has a frontal area of 0.32m x0.3m. Figure 2b shows a photograph of the condenser with an outer tube diameter of 5mm and, inner diameter of 4mm and length of 26.88m, a number of fins 8 fins/cm and total fin area of 7.2m^2, total surface area of 7.38m2. The condenser has a frontal area of 0.6mx0.3m. The compressor has a rated power of 1.7 KW. The system has three capillary tubes with a diameter of 3mm and a length of 50cm.

The system was instrumented to measure temperature, humidity, air flow rate, and power consumption. Six K-type thermocouple temperature sensors were fitted inside the room and the VCR system, as shown in Figure 1. Figure 3 shows the location of the thermocouples fitted on the vapour compression cycle. The thermocouples are connected to a data logger type Picologer TC-08 with temperature accuracy of a Sum of ±0.2% of reading and ±0.5 °C. For measuring air humidity, two Elitech humidity and temperature sensors with accuracy $\pm 3RH$ and ± 0.3 °C with uncertainty of 1.73% are situated at the evaporator suction duct and inside the room. The current input to the compressor was measured using PicoLog® CM3 Current data logger with accuracy (voltage input) $\pm$ 1%. Figure 4 shows photographs of the various measuring devices used. Arduino mega 2560 integrated with a relay kit was used to control the air conditioner compressor for 4 minutes cooling process.
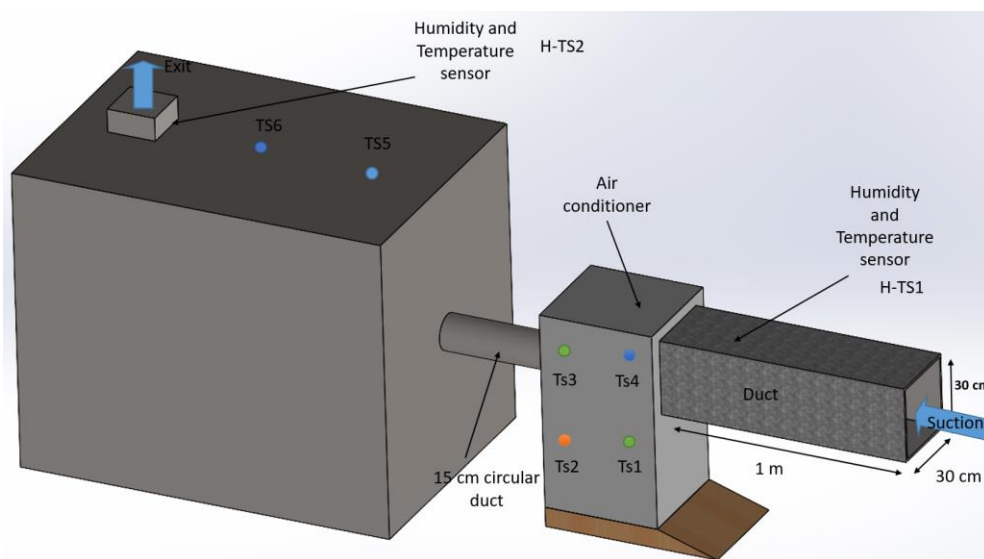
Fig. 1. 3-D system description with sensors locations

(a) (b)

Fig. 2. Evaporator and condenser of the air conditioning system
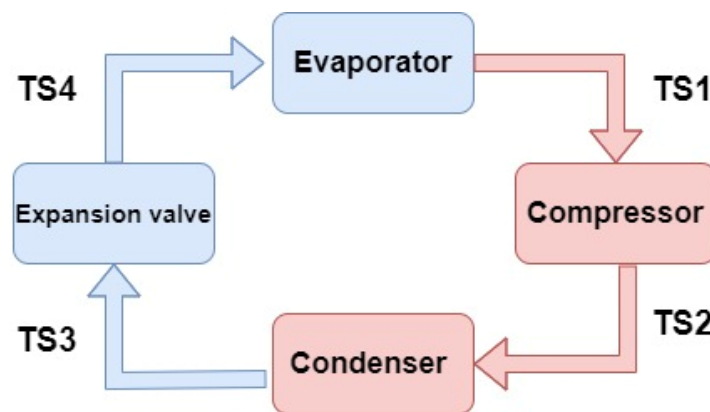
Fig. 3. Sensors distribution inside the cooler
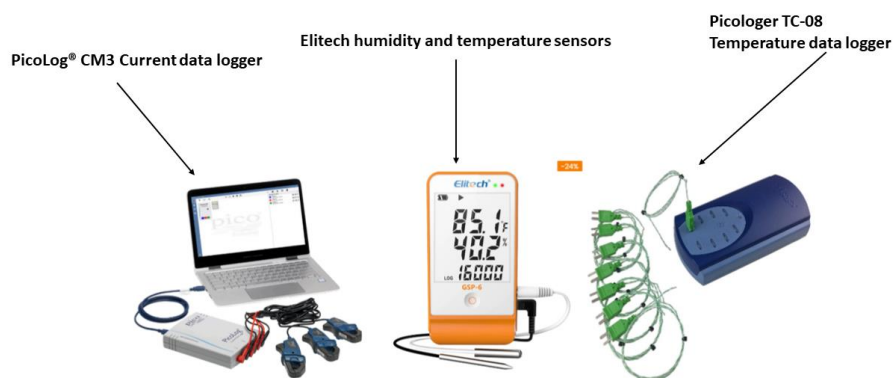
Fig. 4. Measuring sensors

3. Experimental Results

This section presents the experimental results for investigating the effect of ambient temperature and humidity on the air conditioning system performance, including the compressor power consumption, the operating temperatures of the compressor, evaporator and condenser and the room indoor temperature and humidity. Figure 5 shows sample results of testing the air conditioner with an ambient temperature of 23 °C and humidity of 37%. It can be seen that all measured values

have reached steady-state conditions at around 4 minutes. Therefore, this operational time will be the cycle time for the rest of the experiments.
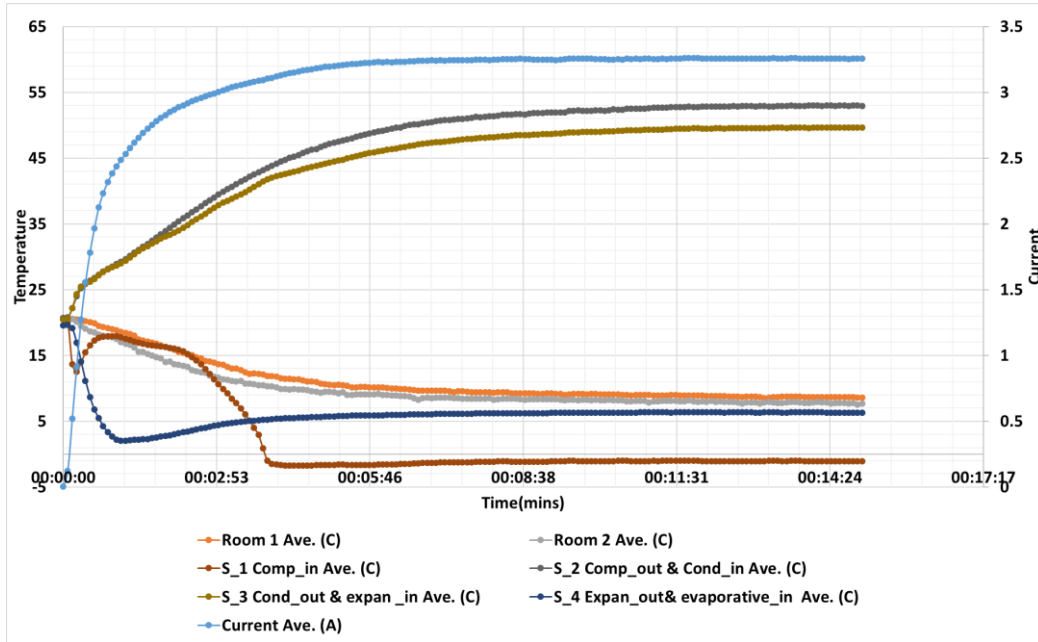
Fig. 5. Full cooling cycle for 15 mins

3.1 Effect of Ambient Temperature

In this section, experimental work was carried out to investigate the effect of increased ambient air temperature on the performance of a vapour compression cooling system while the ambient humidity is constant. Figure 6a shows the effect of ambient temperature on the electric current consumed by the compressor, where the ambient temperature was varied from 22 °C to 27 °C and 40 °C while the air humidity remained constant at 55%. It can be seen that as the ambient temperature increases, the electric current consumed by the compressor increases. Using the current value at the end of 4 minutes, the power consumed based on 240Volts at an ambient temperature of 40 °C is 935.52 Watts, at 27 °C, it is 845.04 Watts, and at 22 °C, it is 751.2 Watts. Therefore, an increase in the power consumption of 184.32 Watts is produced by increasing the temperature by 18 °C, giving 10.24 Watts per 1 degree °C. This increase in power consumption can be explained by the changes to the operating temperature of the various components of the vapour compression cycle, as shown in Figures 6b to 6d. Figure 6b shows that increasing the ambient temperature increased the compressor outlet temperature where at the time of 4 minutes, the compressor temperature increased from 46 °C to 52.5 °C to 59.0 °C when the ambient temperature increased from 22 °C to 27 °C to 40 °C, respectively. Also, figure 6c shows that as the ambient temperature increased, the evaporator temperature increased where when the ambient temperature increased from 22 °C to 27 °C then to 40 °C, the evaporator temperature increased from 6.5 °C to 10.5 °C then to 15 °C respectively. Figure 6d shows the effect of ambient temperature on the condenser temperature which increased from 45 °C to 51.7 °C to 56.9 °C when the ambient temperature increased from 22 °C to 27 °C to 40 °C.
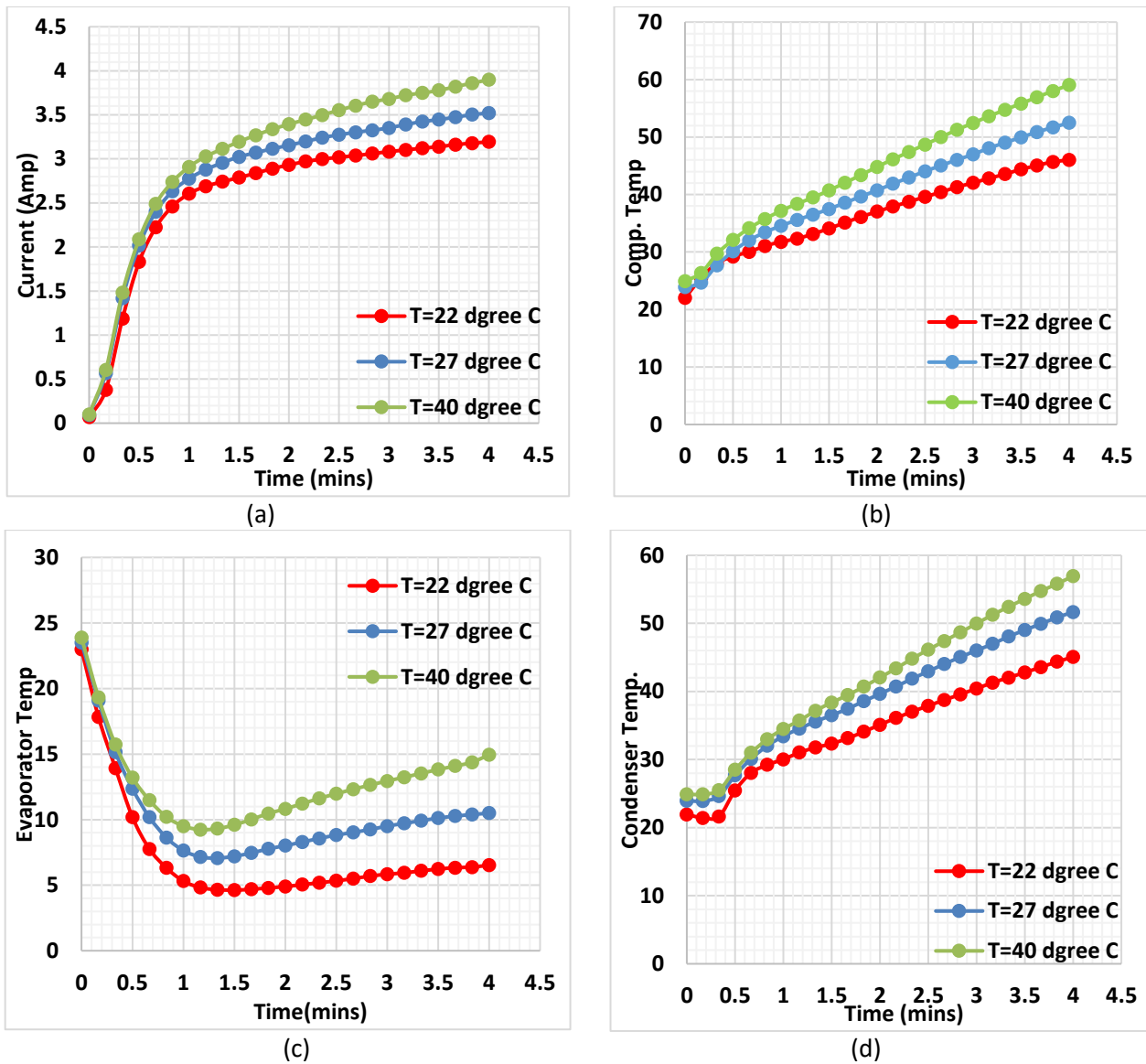
Fig. 6. (a) Effect of input temperature on compressor current consumption at input humidity 55% (b) Effect of input temperature on compressor temperature at input humidity 55% (c) Effect of input temperature on Evaporator temperature at input humidity 55% (d) Effect of input temperature on Evaporator temperature at input humidity 55%

Figure 7 shows the effect of increasing the ambient air temperature on the room indoor temperature and humidity. As the ambient temperature increased from 22 °C to 27 °C, then to 40 °C, the room temperature at the time of 4 minutes increased from 11.8 °C to 17.6 °C then to 21.4 °C as shown in Figure 7a. During the 4 minutes, the change in room temperature decreased significantly due to the increase in the ambient air temperature where at 22 °C, the room temperature changed by 7.8 °C, at 27 °C, the room temperature changed by 5.5°C and at 40 °C the room temperature changed by 2.2 °C. This indicates a significant loss in the cooling capacity of the air conditioner as the ambient air temperature increases. Figure 7b shows the effect of ambient temperature on the room indoor humidity where at 4minutes the humidity increased from 53.2% at ambient temperature of 22 °C to 55.7% at ambient temperature of 27 °C then to 59.4% at ambient temperature of 40 °C. During the testing period of 4minutes, the change in room indoor humidity changed from 7.9% at ambient temperature of 22 °C to 8.2% at ambient temperature of 27 °C, then to 11.3%at ambient temperature of 40 °C.
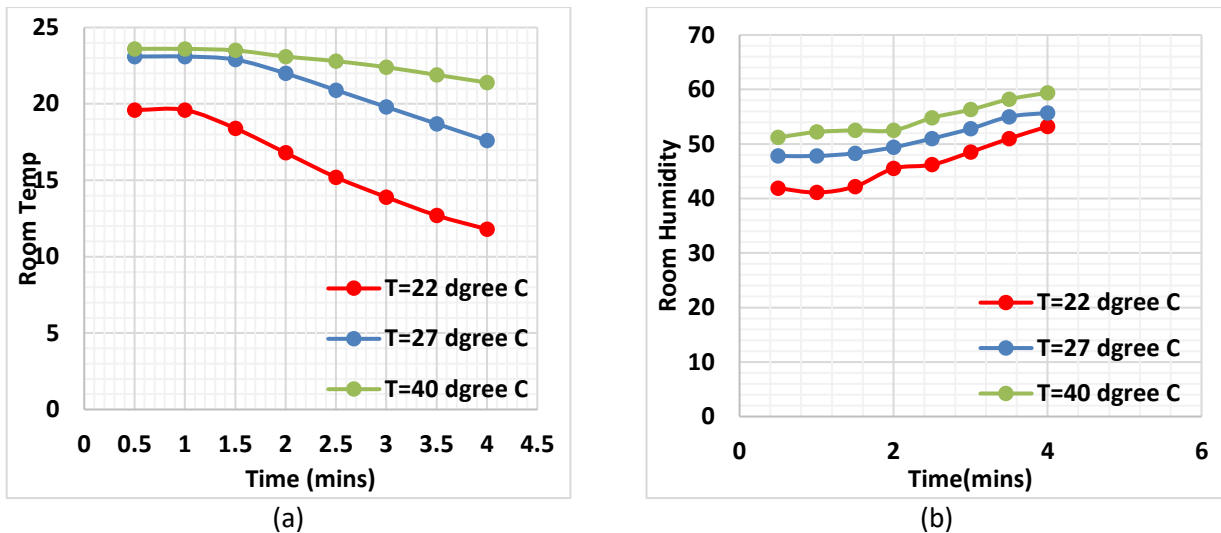
Fig. 7. (a) Effect of input temperature on room temperature at input humidity 55% (b) Effect of input temperature on room humidity at input humidity 55%

3.2 Effect of Ambient Humidity

This section presents experimental work to investigate the effect of changing the ambient humidity on the performance of a vapour compression cooling system while keeping the ambient temperature constant. In the experiments, the humidity varied from 32% to 71% to 88% while the ambient temperature was kept constant at 22 °C. Figure 8a shows the effect of ambient humidity on the electric current consumed by the compressor, showing that as the humidity increases, the current increases. At the time of 4 minutes, the current values increased from 3.08Amps at a humidity of 32% to 3.315Amps at a humidity of 71%, then to 3.555Amps at a humidity of 88%. With a voltage used of 240 volts, the power consumed is 739.2 Watts at 32% humidity, 795.6 Watts at 71% humidity and 853.2 Watts at 88% humidity. Therefore, with the increase of humidity from 32% to 88%, the power consumed increased by 114 Watts.

Figures 8 b, c, and d show the effect of changing the humidity on the operating temperature of the various components of the vapour compression system, namely the compressor outlet temperature, the evaporator temperature and the condenser temperature. Figure 8b shows the effect of varying the humidity from 32% to 71% and then to 88% while the ambient temperature is kept constant at 22 °C on the compressor outlet temperature. At 4 minutes, the compressor outlet temperature increased from 43.8 °C at a humidity of 32% to 48.75 °C at a humidity of 71%, then to 52.49 °C at a humidity of 88%. Similarly, Figure 8c shows that the evaporator temperature increased by increasing the ambient humidity where at the time of 4 minutes, it increased from 5.25 °C at a humidity of 32% to 8.87 °C at a humidity of 71% and then to 10.1 °C at a humidity of 88%. Figure 8d shows that the condenser temperature increases with the increase in ambient humidity where at the time of 4 minutes, it increased from 43.2 °C at a humidity of 32% to 46.4 °C at a humidity of 71% and then to 50.7 °C at a humidity of 88%.

(a)   (b)
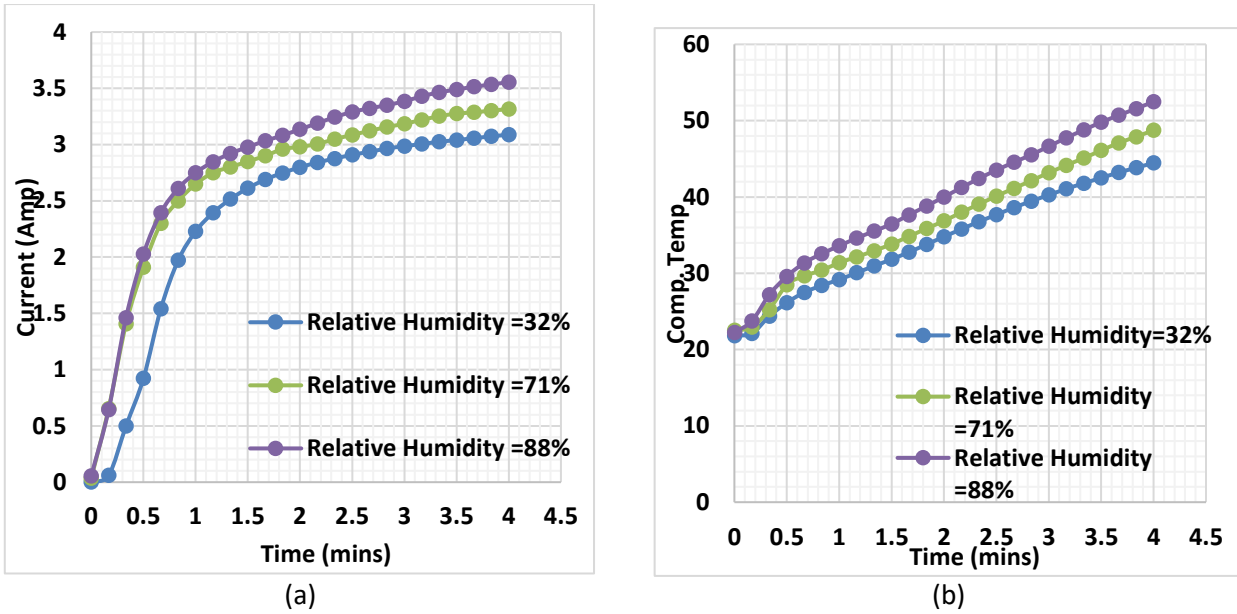
Fig. 8. (a) Effect of input relative humidity on compressor current at input temperature 22 °C (b) Effect of input relative humidity on condenser temperature at input temperature 22 °C

Figure 9 shows the effect of varying the ambient humidity of the room indoor temperature and humidity. Figure 9a shows that as the ambient humidity increases from 32% to 71% to 88% while the ambient temperature is constant at 22 °C, the room indoor temperature at the time of 4 minutes increased from 11 °C to 16 °C then to 19.2 °C respectively. However, the room temperature change during the 4 minutes decreased from 9 °C at a humidity of 32% to 5.3 °C at a humidity of 71%, then to 3.6 °C at a humidity of 88%. Therefore, it is clear that there is a loss in the cooling capacity due to the increase in ambient humidity. Figure 9b shows that as the ambient humidity increases, the room indoor humidity increases. At 4 minutes, it increased from 41.5% at ambient humidity of 32% to 64.4% at ambient humidity of 71% to 69.8% at ambient humidity of 88%. As for the change in room indoor humidity over the testing period of 4 minutes, it changed from 3.9% at ambient humidity of 32% to 9.9% at ambient humidity of 71%, then to 10.5% at ambient humidity of 88%.

(a)   (b)
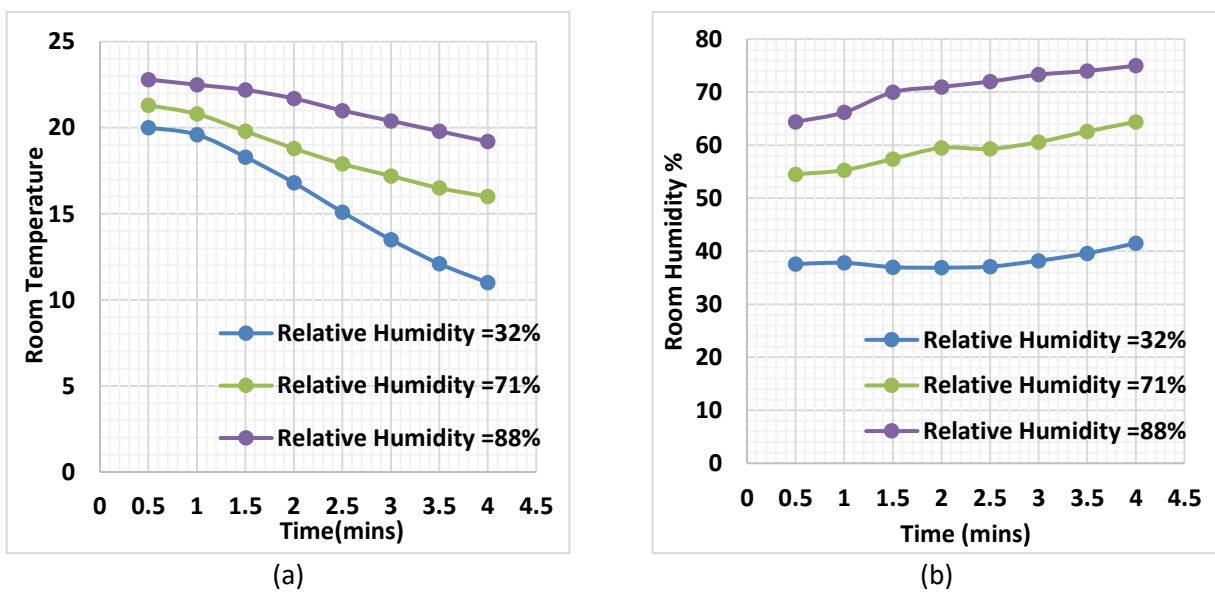
Fig. 9. (a) Effect of input relative humidity on room temperature at input temperature 22 °C (b) Effect of input relative humidity on room humidity at input temperature 22 °C

4. Computational Fluid Dynamic Simulation of the Air-Conditioned Room

This section describes the CFD modelling carried out for the cooled volume shown in Figure 1. The cooled volume is a room of 2 m3 with one inlet for the cold air flow and one outlet with a 0.2m×0.2m cross-section, as shown in Figure 10. The 3-D model was developed using COMSOL multiphysics to predict the room humidity and temperature variation with time. The modules used in this model are Turbulent flow (k-ω) and heat transfer in fluids. Eq. (1) represents the Navier-Stokes equation, which describes the conservation of momentum in the fluid.
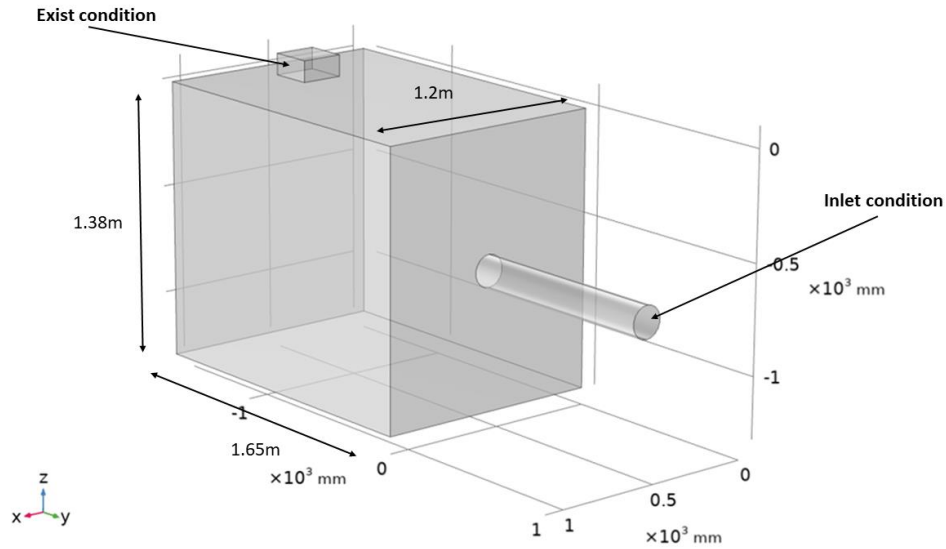
Fig. 10. CFD model configuration

$$\rho(U.\nabla)U = \nabla.[\rho I + K] + F + \rho g \tag{1}$$

Eq. (2) is the continuity equation, which states that the divergence of the velocity vector multiplied by density is zero.

$$\nabla.(\rho U) = 0 \tag{2}$$

Eq. (3) represents the transport equation for turbulent kinetic energy K, where μ is the dynamic viscosity.

$$K = (\mu + \mu T)(\nabla U + (\nabla U)^T) - \frac{2}{3}(\mu + \mu T)(\nabla.U)I - \frac{2}{3}\rho K I \tag{3}$$

Eq. (4) represents the transport equation for the turbulent kinetic energy dissipation rate, where σ_k^* is the turbulent Prandtl number for K.

$$\rho(U.\nabla)K = \nabla.[(\mu + \mu_T\sigma_k^*)\nabla K] + P_K + \beta_0^*\rho\omega K \tag{4}$$

Eq. (5) represents the transport equation for the specific dissipation rate ω, where σ_ω is the turbulent Prandtl number for ω, α is a constant, and β_0^* is a model constant.

$$\rho(U.\nabla)\omega = \nabla.[(\mu + \mu_T \sigma_\omega)\nabla\omega] + \alpha\frac{\omega}{K}P_K - \beta_0^* \rho\omega^2 \,,\, \omega = 0m \tag{5}$$

Eq. (6) defines the turbulent viscosity μ_T, which is related to the turbulent kinetic energy K and the specific dissipation rate ω.

$$\mu_T = \rho\frac{K}{\omega} \tag{6}$$

Eq. (7) represents the production term of turbulent kinetic energy K.

$$\rho_K = \mu_T.[\nabla U : (\nabla U + (\nabla U)^T) - \frac{2}{3}(\nabla.U)^2] - \frac{2}{3}\rho K\nabla.U \tag{7}$$

Eq. (8) represents the energy conservation equation (also known as the heat equation) for a fluid, where the left-hand side represents the advection and diffusion of heat, and the right-hand side represents the heat sources or sinks.

$$\rho C_p U\nabla T + \nabla.q = Q + Q_p + Q_{vd} \tag{8}$$

Eq. (9) represents Fourier's law of heat conduction, where Q is the heat flux vector, and K is the thermal conductivity of the fluid.

$$Q = -K\nabla T \tag{9}$$

Eq. (10) defines the Reynolds number, which is a dimensionless quantity used to characterise the flow regime in a fluid. It is defined as the ratio of inertial forces to viscous forces, where U is the mean velocity, L is the characteristic length, and v is the kinematic viscosity.

$$R_e = \frac{UL}{v} \tag{10}$$

Eq. (11) defines the Grashof number, which is a dimensionless quantity used to predict the occurrence of natural convection in a fluid. It is defined as the ratio of buoyancy forces to viscous forces, where g is the acceleration due to gravity, α is the thermal expansion coefficient, ΔT is the temperature difference, L is the characteristic length, and v is the kinematic viscosity.

$$G_r = \frac{g\alpha\Delta T L^3}{v^2} \tag{11}$$

All physics were coupled and solved numerically using a time-dependent solver, which solves the equations simultaneously to give accurate results with minimum solving iteration time for the non-linear equations. The initial boundary conditions are set by assuming a room temperature of 25 °C and relative humidity of 55%. During the four-minute cooling process, the energy equation and Navier stocks equation were solved to predict the final state of air inside the cooling space using the inputs listed in Table 1.

Table 1
The parameters used in the model

Parameters	Value
Room height(H)	1.38[m]
Room depth (D)	1.65[m]
Room width (W)	1.2[m]
Source inlet velocity(Us)	2.2[m/s]
Outside temperature (Tout)	20[degC]
Source air temperature(Tsource)	10.5[degC]
Wall heat transfer coefficient(h)	0.17[W/(m^2*K)]

(a)

(b)
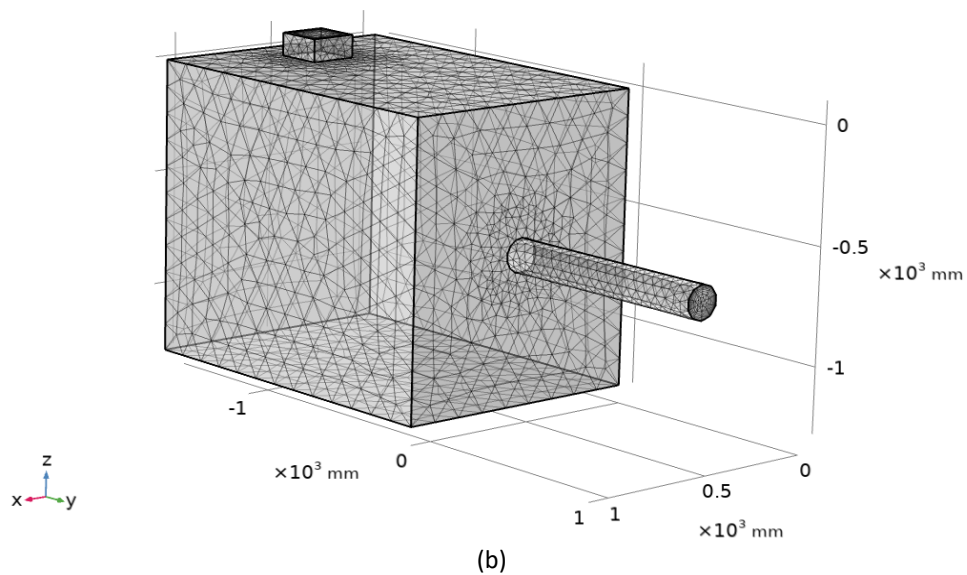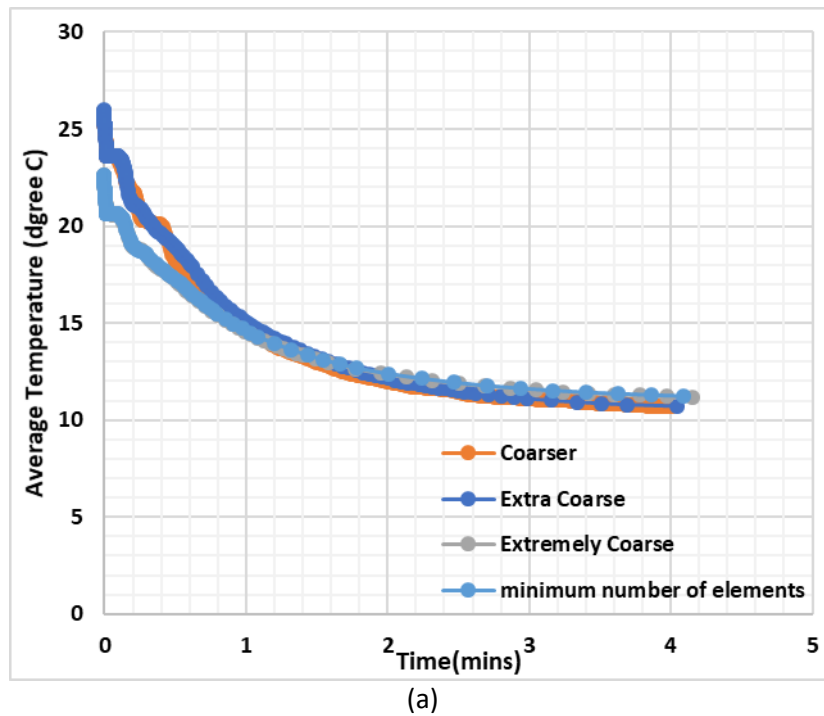
Fig. 11. (a) The mesh sensitivity (b) Mesh distribution in the modelled volume

A mesh sensitivity test was conducted in COMSOL using different sizes of tetrahedron elements mesh: Minimum number of elements, Extremely Coarse, Extra Coarse and Coarser. Table 2 shows

the element count for each mesh size, and Figure 11a illustrates the temperature variation over time. The Extra coarse mesh option produced similar results to the coarser mesh size but with a shorter computational time of 133 minutes. In the other two cases, the maximum deviation error was 15 %. Therefore, a coarser mesh size was used in the simulations, as shown in Figure 11b and they were performed on a PC with an Intel Core i7 processor, 48 GB RAM, and a 1 TB SSD Hard Drive. The first simulation case was run with air inlet conditions of 22 °C and 55% relative humidity, and the room's initial temperature was 19.6 °C and 41.9% relative humidity.

Table 2
Mesh sensitivity analysis

Mesh size	Domain elements	Boundary elements	Edge elements	Simulation time (min)	Mesh size
Coarser	71550	5662	338	2 hours, 41 minutes, 54 seconds	Coarser
Extra coarse	31127	2936	238	28 minutes, 3 seconds	Extra coarse
Extremely coarse	11331	1178	146	13 minutes, 17 seconds	Extremely coarse
Minimum number of elements	10427	1096	139	11 minutes, 40 seconds	Minimum number of elements

Figure 12a and b compares the predicted room temperature and humidity from the CFD simulation with those measured experimentally at 22 °C and 55% humidity, showing good agreement with maximum deviations of 7.6% and 6.2%, respectively. Four consecutive repetitive experiments were performed in the hot room, covering each of the four minutes. Four tests were conducted to assess the repeatability of the temperature measurements within a controlled room environment, each spanning a four-minute duration. During these tests, temperature changes were closely monitored using precision instruments. The objective was to evaluate the consistency of temperature readings over multiple runs. To maintain repeatability, a maximum allowable deviation error of 14.7% was set as the tolerance threshold. This rigorous testing process helps ensure the reliability and accuracy of temperature data collection, which is crucial for maintaining the desired environmental conditions within the room, as seen in Figure 12c.

(a)
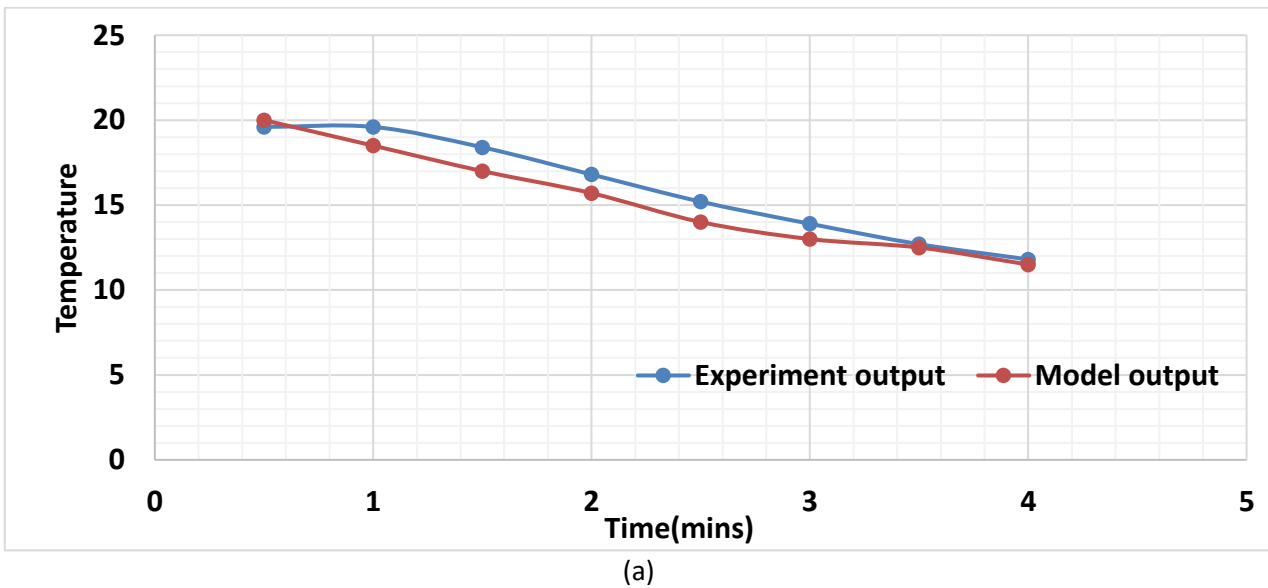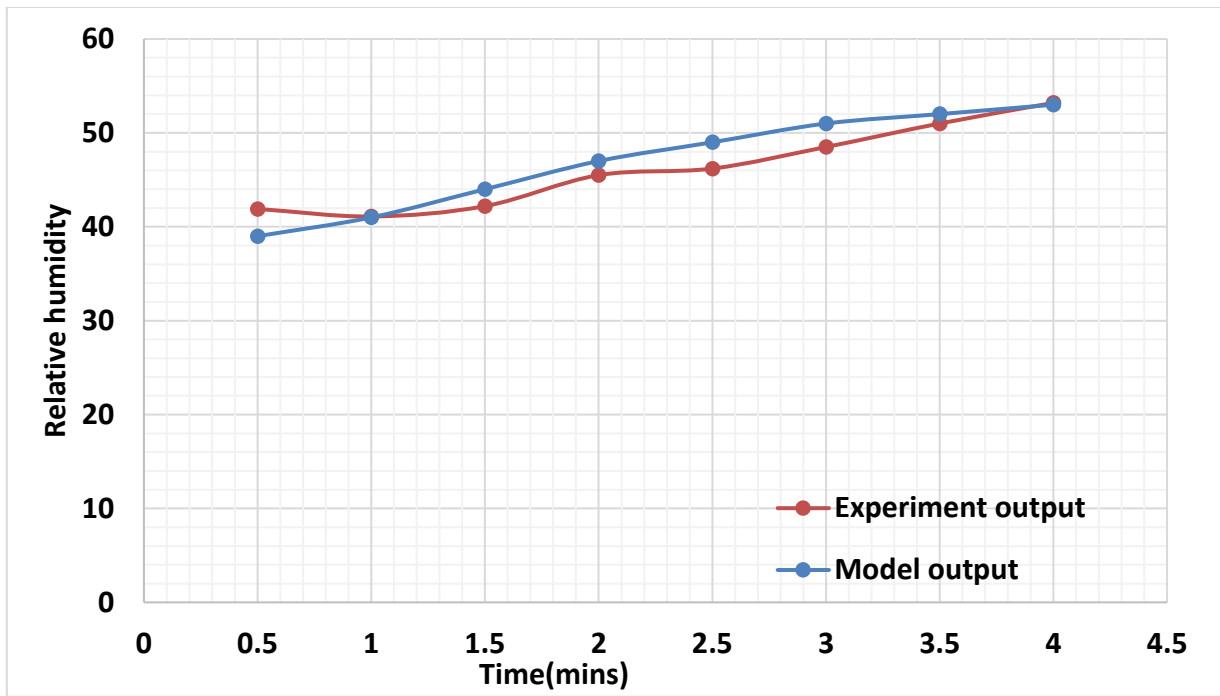
(b)
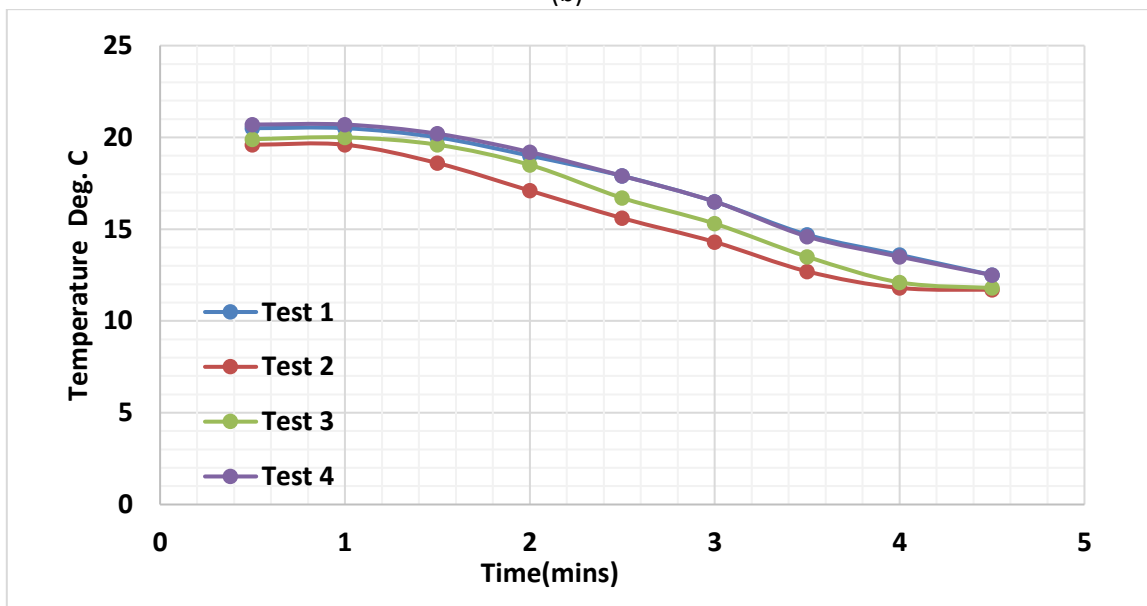
(c)

Fig. 12. (a) Comparison of the model and experimental results for the room temperature variation with time (b) Comparison of the model and experimental results for the room relative humidity variation with time (c) Comparison of the experimental results for the room Temperature variation with time

Figure 13a shows the 3D velocity, temperature and humidity distribution within the cooled space after 4 minutes of simulation at ambient temperature of 22 °C and 55% relative humidity while figure 13b shows the same at ambient conditions of 40 °C and 55% relative humidity.

(a)

(b)
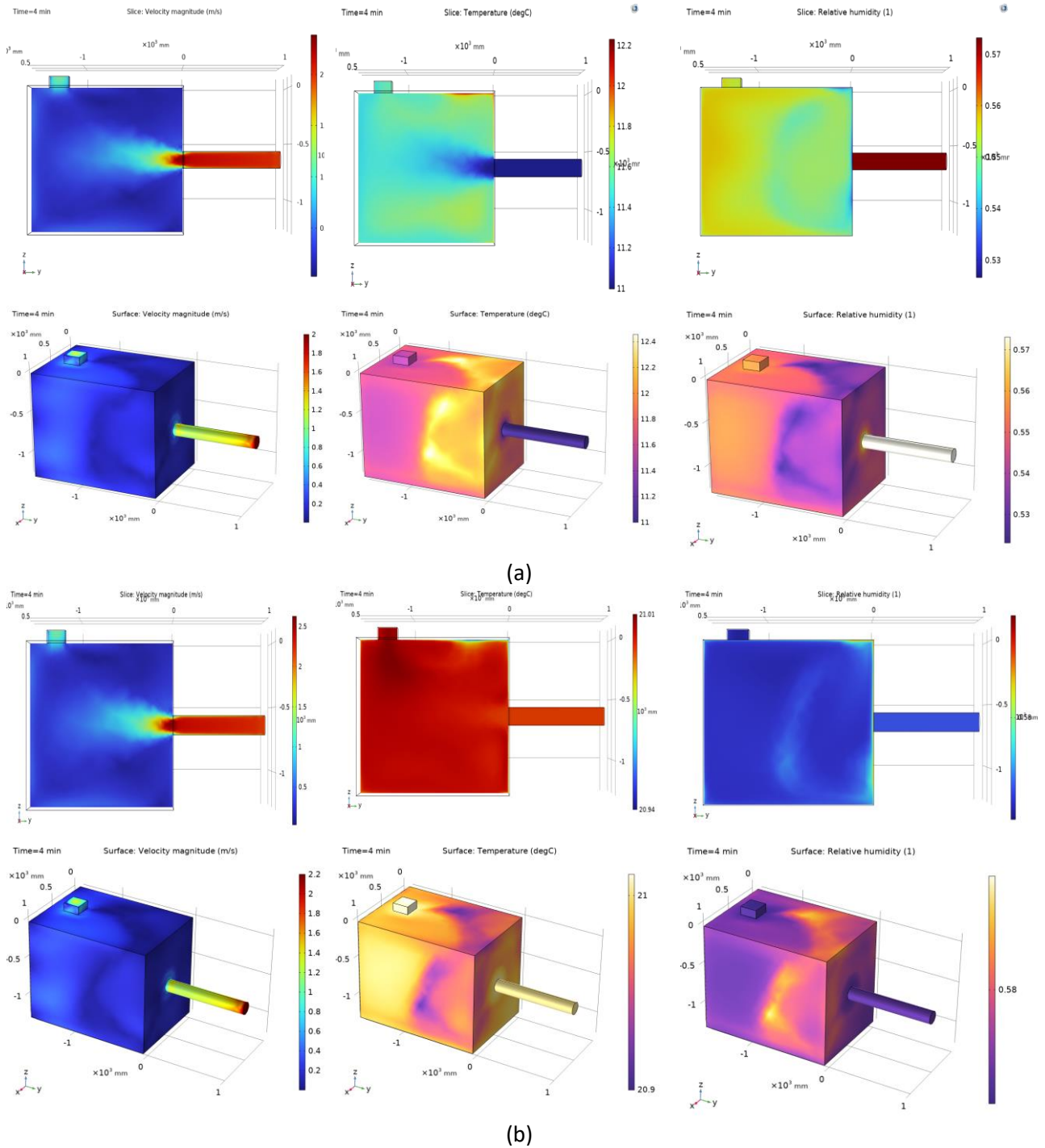
Fig. 13. (a) Predicted velocity, temperature and humidity distribution in the cooled room after 4 minutes at air inlet of 22 °C and 55% relative humidity (b) Predicted velocity, temperature and humidity distribution in the cooled room after 4 minutes at air inlet of 40 °C and 55% relative humidity

Figure 14a shows the 3D velocity, temperature, and humidity distribution within the cooled space after 4 minutes of simulation at ambient conditions of 22 °C and 32% relative humidity while figure 14b shows the same parameters at ambient conditions of 22 °C and 88% relative humidity.

(a)

(b)
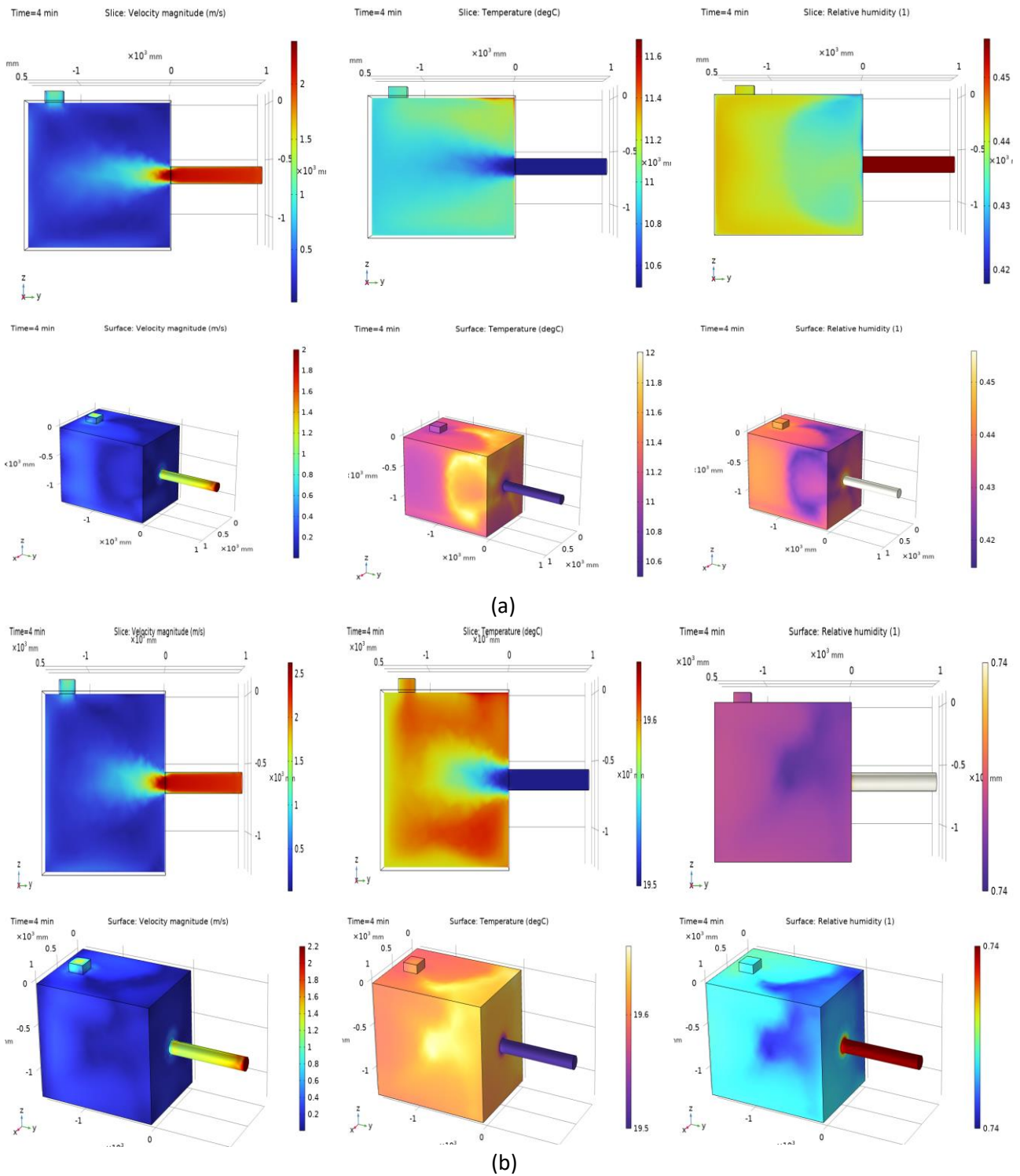
Fig. 14. (a) Predicted velocity, temperature, and humidity distribution in the cooled room after 4 minutes at air inlet of 22 °C and 32% relative humidity (b) Predicted velocity, temperature, and humidity distribution in the cooled room after 4 minutes at air inlet of 22 °C and 88% relative humidity

Figure 15a shows the time enthalpy variation of the air in the room for the operating conditions associated with 22 °C, 55% and 40 °C, 55% ambient conditions. This enthalpy change indicates the amount of cooling achieved during the 4 minutes at these operating conditions. At ambient temperature of 22 °C, the change in enthalpy of the room over the 4 minutes is 11.7kJ/kg.d.a while at ambient temperature of 40 °C, it is 3.6kJ/kg.d.a. This shows that the amount of cooling decreased

as the ambient temperature increased, indicating that the air conditioning system did not deliver the required cooling rate to maintain the room temperature as the ambient temperature increases.

Figure 15b shows the time enthalpy variation of the air in the room for the operating conditions associated with 22 °C, 32% and 22 °C, 88% ambient conditions. At relative humidity of 32%, the change in enthalpy of the room air is 12.857kJ/kg.d.a while at relative humidity of 88%, it is 5.524kJ/kg.d.a. This enthalpy change shows that as the ambient relative humidity increases, the room air enthalpy change decreases indicating that the ability of the air conditioning system to maintain the required cooling capacity is significantly reduced.
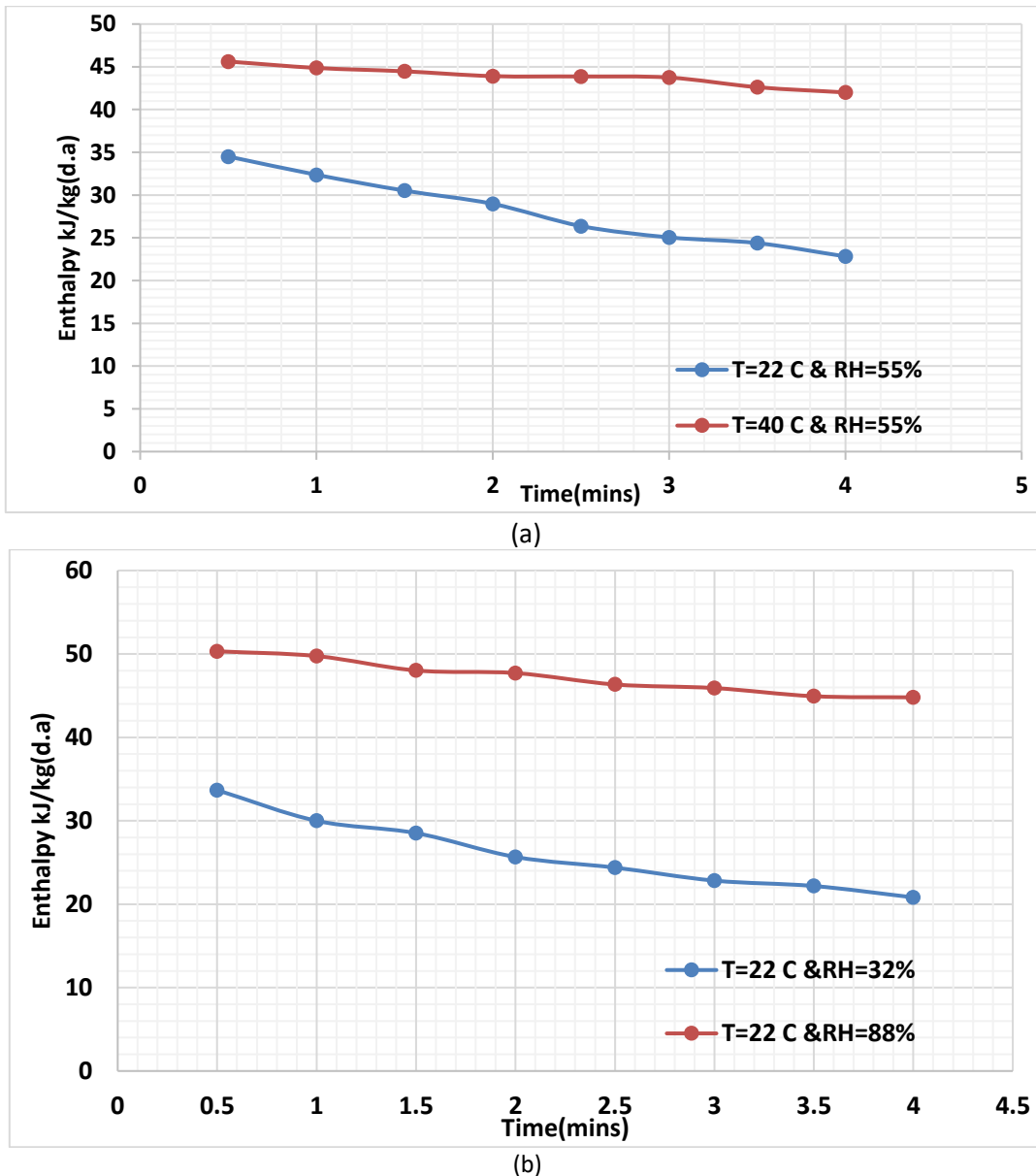
Fig. 15. (a) Room enthalpy variation with time at ambient temperatures of 22 °C and 40 °C and constant relative humidity of 55% (b) Room enthalpy variation with time at ambient relative humidity of 32 °C and 88% and constant temperature of 22 °C

5. Conclusions

Globally, demands for space cooling has significantly increased due to rising temperatures, population growth and urbanisation. To meet these cooling demands, mechanical vapour

compression cooling (VCC) systems are most used over other cooling technologies. VCC technology is relatively mature and well-understood, but with intensive energy consumption and environmental issues due to the refrigerants used that have high global warming potential. Also, ambient temperature and humidity have significant effects on the performance of vapour compression systems, particularly in air conditioning and refrigeration applications in terms of cooling capacity and power consumption. Therefore, this paper experimentally and numerically investigates the impact of ambient temperature and humidity on the performance of vapour compression air conditioning system in terms of power consumption and cooling capacity. The following conclusions can be drawn:

i. At ambient humidity of 55%, as the ambient temperature increases from 22 to 40 °C, the compressor temperature has increased from 46 °C to 59 °C at the 4 minutes run. This resulted in increasing the power consumption of the air conditioning system from 751.2 to 935.52 Watts, an increase of 184.32 Watts is produced by increasing the temperature by 18 °C giving 10.24 Watts per 1 degree °C.

ii. As for the evaporator and condenser temperatures, results showed that increasing the ambient temperature from 22 to 40 °C while the humidity kept at 55%, the evaporator temperature increased from 6.5 to 15 °C while the condenser temperature increased from 45 °C to 56.9 °C. As the evaporator and condenser temperatures increase, their heat transfer performance decreases, therefore reducing the system overall performance. Particularly, increasing the evaporator temperature leads to the increase in the temperature of air to be delivered to the cooled space thus reducing its ability to maintain the room temperature at the required comfort conditions.

iii. Also, it was observed that as the ambient relative humidity increased, the performance of the VCC air conditioning system deteriorated. At an ambient temperature of 22 °C, increasing the ambient relative humidity from 32% to 88% resulted in increasing the compressor temperature from 43.8 °C. This led to increasing the air conditioning system power consumption from 739.2 Watts to 853.2 Watts, an increase of 114 Watts. Also, increasing the ambient humidity resulted in increasing the evaporator temperature from 5.25 °C at a humidity of 32% to 10.1 °C at humidity of 88%. Similarly, the condenser temperature increased from 43.2 °C at humidity of 32% to 50.7 °C at a humidity of 88%. The increase in the evaporator and condenser temperatures as the ambient humidity increases led to reducing the heat transfer performance of these heat exchangers and the performance of the air conditioning system.

iv. Regarding the room air temperature and humidity, it was observed that increasing the ambient temperature resulted in an increase in the room indoor temperature and humidity. At humidity of 55%, increasing the ambient temperature from 22v to 40 °C resulted in reducing the room temperature change (cooling) from 7.8K to 2.2K respectively. Also, increasing the ambient temperature from 22 to 40 °C resulted in increasing the change in the room air humidity from 7.9% to 11.3%. Similarly, as the ambient humidity increased from 32% to 88% while the ambient temperature remained constant at 22 °C, the change in the room air temperature decreased from 9K to 3.6K while the change in room air humidity increased from 3.9% to 10.5%.

v. Computational fluid dynamic simulation is a powerful tool to predict the performance of thermal systems. In this work, a validated CFD model was developed for the cooled space and predicted its temperature and humidity with maximum deviation of 7.6% and 6.2% respectively. This model was used to predict the air enthalpy change inside the room showing that as the ambient temperature increased from 22 °C to 40 °C at relative humidity of 55%,

the enthalpy change decreased 11.7kJ/kg.d.a to 3.6kJ/kg.d.a. While increasing the ambient relative humidity from 32% to 88% at constant temperature of 22 °C resulted in decreasing the enthalpy change from 12.857kJ/kg.d.a to 5.524kJ/kg.d.a. Therefore, increasing the ambient temperature and humidity led to significant loss in the cooling provision for the room.

vi. This work highlighted the adverse effects of ambient temperature and humidity on the performance of vapour compression air conditioning systems in terms of increased power consumption and the loss of cooling capacity.

Acknowledgement

Conflicts of Interest

The authors declare no conflict of interest.

References

[1] "International Energy Agency (IEA), Perspectives for the clean energy transition," *Sustainable Energy Technologies and Assessments*. 2021.

[2] T. Uk, "Sustainable cooling," no. 642, pp. 1–8, 2021, [Online].

[3] Sajjad, Uzair, Naseem Abbas, Khalid Hamid, Saleem Abbas, Imtiyaz Hussain, Syed Muhammad Ammar, Muhammad Sultan, Hafiz Muhammad Ali, Muzamil Hussain, and Chi Chuan Wang. "A review of recent advances in indirect evaporative cooling technology." *International Communications in Heat and Mass Transfer* 122 (2021): 105140. https://doi.org/10.1016/j.icheatmasstransfer.2021.105140

[4] Jacob, Tabeel A., Nihar Shah, and Won Young Park. "Evaluation of hybrid evaporative-vapor compression air conditioners for different global climates." *Energy Conversion and Management* 249 (2021): 114841. https://doi.org/10.1016/j.enconman.2021.114841

[5] Shah, Surendra H., Kalash R. Pai, Sachin R. Shinde, and Bhaskar N. Thorat. "Analysis of a vapor compression refrigeration system using a fog-cooled condenser." *Applied Thermal Engineering* 196 (2021): 117299. https://doi.org/10.1016/j.applthermaleng.2021.117299

[6] Kulkarni, Sourabh, Shriramshastri Chavali, and Shruti Dikshit. "A review on analysis of Vapour Compression Refrigeration System (VCRS) for its performance using different ecofriendly refrigerants and nanofluids." *Materials Today: Proceedings* 72 (2023): 878-883. https://doi.org/10.1016/j.matpr.2022.09.085

[7] Mahmood, R. A., O. M. Ali, A. Al-Janabi, G. Al-Doori, and M. M. Noor. "Review of mechanical vapour compression refrigeration system part 2: performance challenge." *International Journal of Applied Mechanics and Engineering* 26, no. 3 (2021): 119-130. https://doi.org/10.2478/ijame-2021-0039

[8] Franco, S. S., J. R. Henríquez, A. A. V. Ochoa, J. A. P. Da Costa, and K. A. Ferraz. "Thermal analysis and development of PID control for electronic expansion device of vapor compression refrigeration systems." *Applied Thermal Engineering* 206 (2022): 118130. https://doi.org/10.1016/j.applthermaleng.2022.118130

[9] Shah, Nihar, Max Wei, Virginie Letschert, and Amol Phadke. *Benefits of energy efficient and low-global warming potential refrigerant cooling equipment*. No. LBNL-2001229. Lawrence Berkeley National Lab.(LBNL), Berkeley, CA (United States), 2019. https://doi.org/10.2172/1559243

[10] Cengel, Yunus A., Michael A. Boles, and Mehmet Kanoğlu. *Thermodynamics: an engineering approach*. Vol. 5. New York: McGraw-hill, 2011.

[11] Alawadhi, Mubarak, and Patrick E. Phelan. "Review of Residential Air Conditioning Systems Operating under High Ambient Temperatures." *Energies* 15, no. 8 (2022): 2880. https://doi.org/10.3390/en15082880

[12] Bezerra, Paula, Fabio da Silva, Talita Cruz, Malcolm Mistry, Eveline Vasquez-Arroyo, Leticia Magalar, Enrica De Cian, André FP Lucena, and Roberto Schaeffer. "Impacts of a warmer world on space cooling demand in Brazilian households." *Energy and Buildings* 234 (2021): 110696. https://doi.org/10.1016/j.enbuild.2020.110696

[13] Cao, Jingfu, Mingcai Li, Min Wang, and Bojia Li. "Impacts of temperature and humidity changes on air-conditioning design load under the climate change conditions in different climate zones of China." *Meteorological Applications* 28, no. 5 (2021): e2026. https://doi.org/10.1002/met.2026

[14] Ambarita, H., A. Halim Nasution, S. Ginting, and H. V. Sihombing. "The optimum temperature of single-stages vapor compression refrigeration cycle for Air-Conditioning unit." In *IOP Conference Series: Materials Science and Engineering*, vol. 420, no. 1, p. 012038. IOP Publishing, 2018. https://doi.org/10.1088/1757-899X/420/1/012038

[15] Zaidan, Maki H., Thamir K. Ibrahim, and Aadel AR Alkumait. "Performance enhancement by using wet pad in vapor compression cooling system." *Journal of Engineering and Technological Sciences* 51, no. 1 (2019): 48-63. https://doi.org/10.5614/j.eng.technol.sci.2019.51.1.4

[16] Mitrakusuma, Windy H., Apip Badarudin, Hafidz Najmudin, and Andriyanto Setyawan. "Performance of split-type air conditioner under varied outdoor air temperature at constant relative humidity." *Journal of Advanced Research in Fluid Mechanics and Thermal Sciences* 90, no. 2 (2021): 42-54. https://doi.org/10.37934/arfmts.90.2.4254

[17] Yusof, Mohd Hazwan, Sulaiman Mohd Muslim, Muhammad Fadhli Suhaimi, and Mohamad Firdaus Basrawi. "The effect of refrigerant charge and outdoor temperature on the condenser and evaporator of a split-unit type air conditioner using R22 refrigerant." In *MATEC Web of Conferences*, vol. 225, p. 02013. EDP Sciences, 2018. https://doi.org/10.1051/matecconf/201822502013

[18] Setyawan, Andriyanto, Hafid Najmudin, Apip Badarudin, and Cecep Sunardi. "Evaluation of Split-Type Air Conditioner Performance under Constant Outdoor Moisture Content and Varied Dry-Bulb Temperature." *International Journal of Heat & Technology* 40, no. 5 (2022). https://doi.org/10.18280/ijht.400521

[19] Yau, Y. H., and H. L. Pean. "The performance study of a split type air conditioning system in the tropics, as affected by weather." *Energy and buildings* 72 (2014): 1-7. https://doi.org/10.1016/j.enbuild.2013.12.010

[20] Yau, Y. H., and H. L. Pean. "The performance study of a split type air conditioning system in the tropics, as affected by weather." *Energy and buildings* 72 (2014): 1-7. https://doi.org/10.1016/j.enbuild.2013.12.010

[21] Khalifa, Abdul Hadi N., Johain J. Fataj, and Ali K. Shaker. "Performance study on a window type air conditioner condenser using alternative refrigerant R407C." *Engineering Journal* 21, no. 1 (2017): 235-243. https://doi.org/10.4186/ej.2017.21.1.235

[22] Setyawan, Andriyanto, Susilawati Susilawati, Tandi Sutandi, and Hafid Najmudin. "Performance of Air Conditioning Unit under Constant Outdoor Wet-Bulb Temperature and Varied Dry-Bulb Temperature." *International Journal of Heat & Technology* 39, no. 5 (2021). https://doi.org/10.18280/ijht.390510

[23] Bilgili, M. E. H. M. E. T., A. Ozbek, A. Yasar, E. Simsek, and B. Sahin. "Effect of atmospheric temperature on exergy efficiency and destruction of a typical residential split air conditioning system." *International Journal of Exergy* 20, no. 1 (2016): 66-84. https://doi.org/10.1504/IJEX.2016.076679

[24] Ding, Yanjun, Qinhu Chai, Guoyuan Ma, and Yi Jiang. "Experimental study of an improved air source heat pump." *Energy Conversion and Management* 45, no. 15-16 (2004): 2393-2403. https://doi.org/10.1016/j.enconman.2003.11.021

[25] Wang, Xudong, Yunho Hwang, and Reinhard Radermacher. "Two-stage heat pump system with vapor-injected scroll compressor using R410A as a refrigerant." *International Journal of Refrigeration* 32, no. 6 (2009): 1442-1451. https://doi.org/10.1016/j.ijrefrig.2009.03.004

[26] Guo, Weihua, GaoFeng Ji, Honghong Zhan, and Dan Wang. "R32 Compressor for Air conditioning and Refrigeration applications in China." (2012).

[27] J. J. Abdulhameed, M. S. Kassim, and M. S. Kadhim, "Experimental investigation of a condenser air humidity effect on superheated degree of compressor," *J. Mech. Eng. Res. Dev.*, vol. 44, no. 5, pp. 167–176, 2021.

[28] Abdelgaied, Mohamed, Mohamed A. Saber, Mohamed Mahgoub Bassuoni, and Ahmed M. Khaira. "Adsorption air conditioning: a comprehensive review in desiccant materials, system progress, and recent studies on different configurations of hybrid solid desiccant air conditioning systems." *Environmental Science and Pollution Research* 30, no. 11 (2023): 28344-28372. https://doi.org/10.1007/s11356-023-25209-z

[29] Han, Xing, and Xu Zhang. "Experimental study on a residential temperature–humidity separate control air-conditioner." *Energy and buildings* 43, no. 12 (2011): 3584-3591. https://doi.org/10.1016/j.enbuild.2011.09.029

[30] Sun, Jianting, Zhitao Zuo, Qi Liang, Xin Zhou, Wenbin Guo, and Haisheng Chen. "Theoretical and experimental study on effects of Humidity on Centrifugal compressor performance." *Applied Thermal Engineering* 174 (2020): 115300. https://doi.org/10.1016/j.applthermaleng.2020.115300

[31] S. P. Sonani, B.J., B.J. Sonani, "Effect of Compressor Inlet Temperature and Relative Humidity on Air Liquefaction Cycle Performance .," vol. 2, no. 1979, p. 1979, 2016.

[32] Jani, D. B., Manish Mishra, and Pradeep K. Sahoo. "Performance prediction of rotary solid desiccant dehumidifier in hybrid air-conditioning system using artificial neural network." *Applied Thermal Engineering* 98 (2016): 1091-1103. https://doi.org/10.1016/j.applthermaleng.2015.12.112

[33] Aziz, Andrew N., Raya Al-Dadah, Saad Mahmoud, Mohamed A. Ismail, Mohammed K. Almesfer, Marwa F. El-Kady, and Hassan Shokry. "MOF-801/Graphene Adsorbent Material for Greenhouse Climate Control System—Numerical Investigation." *Energies* 16, no. 9 (2023): 3864. https://doi.org/10.3390/en16093864

[34] Aziz, Andrew N., Saad Mahmoud, Raya Al-Dadah, Mohamed A. Ismail, and Mohammed K. Al Mesfer. "Numerical and experimental investigation of desiccant cooling system using metal organic framework materials." *Applied Thermal Engineering* 215 (2022): 118940. https://doi.org/10.1016/j.applthermaleng.2022.118940

[35] Fahmy, M., M. Morsy, H. Abd Elshakour, and A. M. Belal. "Effect of thermal insulation on building thermal comfort and energy consumption in Egypt." *Journal of Advanced Research in Applied Mechanics* 43, no. 1 (2018): 8-19.